Triple shape coexistence and β decay of ^{96}Y to ^{96}Zr

A. Petrovici* and A. S. Mare
National Institute for Physics and Nuclear Engineering - Horia Hulubei, R-077125 Bucharest, Romania
and Faculty of Physics, University of Bucharest, R-077125 Bucharest, Romania

(Received 19 November 2019; accepted 6 February 2020; published 19 February 2020)

The effects of shape coexistence in ^{96}Y and ^{96}Zr on the β^- first-forbidden decay of the 0^- ground state and Gamow-Teller decay of the 8^+ isomer of ^{96}Y to ^{96}Zr were studied within the beyond-mean-field *complex* excited Vampir model. The structure of the parent and daughter states and the β-decay properties have been investigated using an effective interaction derived from a G matrix based on the charge-dependent Bonn CD potential and a large model space. The influence of shape coexistence and mixing on the properties of the states involved in the investigated allowed and first-forbidden β^- decays is discussed and comparison to the available data is presented.

DOI: 10.1103/PhysRevC.101.024307

I. INTRODUCTION

Neutron-rich nuclei in the $A \approx 100$ mass region relevant for the astrophysical r-process manifest significant variations of particular properties associated with the onset of deformation around the neutron number $N = 58$ [1–11]. Even sudden changes have been identified in some isotopic chains like Sr and Zr, while a smoother transition was observed in the Kr chain. Our previous beyond-mean-field investigations identified triple shape coexistence in the $N = 58$ ^{96}Sr and ^{98}Zr isotopes [5] and oblate-prolate coexistence and mixing in ^{94}Kr [10]. Recently the onset of deformation at $N = 57$ was marked by a new isomer in ^{96}Y [11].

In this work we study new phenomena requiring triple shape coexistence in neutron-rich $A \approx 100$ nuclei with $N = 56, 57$ for a comprehensive description of the identified characteristics at low and intermediate spins. The properties of the states involved in the β^- first-forbidden decay of the 0^- ground state and the Gamow-Teller decay of the 8^+ isomer in ^{96}Y to ^{96}Zr are investigated within the *complex* excited Vampir variational model with symmetry projection before variation using a realistic effective interaction and a large model space.

In the next section the *complex* excited Vampir model, the effective Hamiltonian, and the theoretical formalism for calculating the nuclear matrix elements involved in the investigated allowed and first-forbidden β^- decay will be described. In Sec. III the results concerning the investigated β^- transitions and the triple shape coexistence identified in the structure of the states involved in the decay of the 0^- ground state and the decay of the 8^+ isomeric state of ^{96}Y to ^{96}Zr will be discussed. Finally, some conclusions will be presented in Sec. IV.

II. THEORETICAL FRAMEWORK

The basic building blocks of the *complex* excited Vampir model (EXVAM) are Hartree-Fock-Bogoliubov (HFB) vacua. The corresponding HFB transformations are essentially *complex* and allow the mixing of proton and neutron states as well as different parity and angular momentum states being restricted by time-reversal and axial symmetry. This type of HFB vacua account for arbitrary two-nucleon correlations and thus simultaneously describe like-nucleon as well as isovector and isoscalar proton-neutron pairing including natural- and unnatural-parity two-body correlations. The broken symmetries of the HFB vacua (nucleon numbers, parity, total angular momentum) are restored by projection before variation and the resulting symmetry-projected configurations are used as trial wave functions in chains of successive variational calculations to determine the underlying HFB transformations ([5] and references therein). Finally, the residual interaction between the successively created lowest solutions for each symmetry is diagonalized to determine the mixing of the EXVAM configurations. The beyond-mean-field procedure allows to find in a small excitation energy interval projected configurations manifesting different properties in the intrinsic system. One can identify triple shape coexistence, in particular, spherical, oblate, and prolate deformed configurations successively appearing in the chain of variational calculations underlying the lowest few states of a given symmetry. Projected configurations manifesting significant correlations between them could become strongly mixed in the structure of the wave functions by the final diagonlization. The *complex* excited Vampir model enables the use of rather large model spaces and realistic effective interactions making feasible *large-scale* nuclear structure investigations going far beyond the abilities of the conventional shell-model configuration-mixing approach.

For nuclei in the $A \approx 100$ mass region we used a large model space above the ^{40}Ca core including the $1p_{1/2}$, $1p_{3/2}$,

*spetro@nipne.ro

$0f_{5/2}$, $0f_{7/2}$, $2s_{1/2}$, $1d_{3/2}$, $1d_{5/2}$, $0g_{7/2}$, $0g_{9/2}$, and $0h_{11/2}$ oscillator orbits for both protons and neutrons in the valence space. This model space was successfully used for the description of shape coexistence phenomena revealed by the structure and Gamow-Teller β decay of neutron-rich $A \approx 100$ nuclei [3–6,10,11].

The effective two-body interaction is constructed from a nuclear matter G matrix based on the Bonn CD potential. This G matrix was modified by adding short-range (0.707 fm) Gaussians in the $T = 1$ and $T = 0$ channels in order to enhance the pairing correlations. In addition the isoscalar interaction was modified by monopole shifts for the matrix elements of the form $\langle 0g_{9/2}0f; IT = 0|\hat{G}|0g_{9/2}0f; IT = 0\rangle$ involving protons and neutrons in the $0g_{9/2}$, $0f_{5/2}$, and $0f_{7/2}$ orbitals, influencing the oblate-prolate competition in the investigated nuclei. The Hamiltonian incorporates the two-body matrix elements of the Coulomb interaction between the valence protons. We obtained the wave functions of the 0^- ground state and the 8^+ isomeric state in ^{96}Y including in the excited Vampir many-nucleon bases up to 10 EXVAM configurations. In ^{96}Zr for the description of the 0^+ states we constructed the lowest eight projected configurations, the dimension of the EXVAM basis for the 8^+ states was 45, while for the 7^+ and 9^+ states was 20. The final solutions for each considered state in the parent ^{96}Y and the daughter ^{96}Zr have been obtained diagonalizing the residual interaction between the projected excited Vampir configurations constructed for each spin-parity in independent chains of variational calculations.

We calculated the half-life of the 0^- ground state of ^{96}Y considering the first-forbidden $0^- \rightarrow 0^+$ transitions to the lowest four 0^+ states, while for the 8^+ isomer the Gamow-Teller (GT) strength distributions to 8^+, 7^+, and 9^+ states in ^{96}Zr have been taken into account. The partial half-life of a transition is obtained by

$$\frac{1}{t_{1/2}} = \frac{f}{K} \tag{1}$$

with $K = 6146$ s and the phase factor has the form

$$f = \int_1^{W_0} C(W)W(W^2-1)^{1/2}(W_0 - W)^2 F(Z,W)dW, \tag{2}$$

where $F(Z,W)$ is the Fermi function correcting the phase space integral for the Coulomb distortion of the electron wave function near the nucleus, W is the total, rest mass and kinetic, energy of the electron in units of $m_e c^2$, $\sqrt{W^2-1}$ is the momentum in units of $m_e c$, and W_0 is the maximum electron energy in units of $m_e c^2$.

For the Gamow-Teller transitions the shape factor does not depend on the electron energy and has the form

$$C(W) = B(GT). \tag{3}$$

The GT reduced transition probabilities can be written as

$$B_{if}(GT) = \frac{g_A^2}{2J_i+1}|M_{GT}|^2, \tag{4}$$

where $g_A = 1.26$ and the nuclear matrix elements between the initial ($|\xi_i J_i\rangle$) and the final ($|\xi_f J_f\rangle$) states of spin J_i and J_f,

$$M_{GT} = \sum_{ab} m_{GT}(ab)\langle \xi_f J_f||[c_a^\dagger \tilde{c}_b]_1||\xi_i J_i\rangle, \tag{5}$$

are composed of the reduced single-particle matrix elements of Pauli spin operator $\boldsymbol{\sigma}$, $m_{GT} = \langle a||\boldsymbol{\sigma}||b\rangle$, and the reduced one-body transition densities calculated using the harmonic oscillator wave functions. For β^- decay $c_a^\dagger$ is the proton creation operator and $\tilde{c}_b$ is the neutron annihilation operator and the sum runs over the valence nucleons. Quenching for the axial-vector coupling constant g_A was not applied since we use the same large model space including the spin-orbit partners for both protons and neutrons except the $0h_{9/2}$ spherical orbital. The role played by this orbital for neutron-rich $A \approx 100$ nuclei is under investigation. A missing Gamow-Teller strength of $\approx$10% attributed to the Δ excitation [12] is not included in the present results.

For the first-forbidden transitions of $0^- \rightarrow 0^+$ type the shape factor is

$$C(W) = k + kb/W, \tag{6}$$

where the coefficients k and kb depend on the nuclear first-forbidden matrix elements of rank 0 operators

$$O(0^-) = \sum_{ab} o^{(0)}(0^-)(ab)\langle \xi_f J_f||[c_a^\dagger \tilde{c}_b]_0||\xi_i J_i\rangle. \tag{7}$$

Following Behrens and Bühring [13] and the detailed expressions given in [14,15] the reduced single particle matrix elements occur in the following combinations:

$$k = \zeta_0^2 + \tfrac{1}{9}w^2, \tag{8}$$

$$kb = \tfrac{2}{3}\mu_1\gamma_1[-\zeta_0 w] \tag{9}$$

with

$$\zeta_0 = V + \tfrac{1}{3}wW_0,$$
$$V = v + \xi w'. \tag{10}$$

The parameter $\mu_1 \approx 1$ [16], γ_1 is given by $\sqrt{1-(\alpha Z)^2}$, α is the fine-structure constant, $\xi = \alpha Z/2R$, and R is the nuclear charge radius. The reduced single-particle matrix elements are

$$w = -g_A\sqrt{3}\langle a||r[\boldsymbol{C}_1 \times \boldsymbol{\sigma}]^{(0)}||b\rangle, \tag{11}$$

$$w' = -g_A\sqrt{3}\langle a||\tfrac{2}{3}rI(1,1,1,1,r)[\boldsymbol{C}_1 \times \boldsymbol{\sigma}]^{(0)}||b\rangle, \tag{12}$$

$$v = \frac{\epsilon_{\rm mec} g_A\sqrt{3}}{M}\langle a||[\boldsymbol{\sigma} \times \boldsymbol{\nabla}]^{(0)}||b\rangle, \tag{13}$$

where

$$\boldsymbol{C}_{lm} = \sqrt{\frac{4\pi}{2l+1}}\boldsymbol{Y}_{lm} \tag{14}$$

with $\boldsymbol{Y}_{lm}$ the spherical harmonics, M is the nucleon mass, and the Coulomb factor taking into account the nuclear charge distribution approximated by a uniform spherical distribution

TABLE I. The structure of the wave functions for the lowest four 0^+ states of ^{96}Zr.

$I[\hbar]$	Spherical	Prolate	Oblate
0_1^+	94%	1%	4%
0_2^+	19%	45%	35%
0_3^+	30%	54%	15%
0_4^+	36%	16%	47%

is given by [16]

$$I(1,1,1,1,r) = \frac{3}{2}\begin{cases} 1-\frac{1}{5}\left(\frac{r}{R}\right)^2 & 0 \leqslant r \leqslant R, \\ \frac{R}{r}-\frac{1}{5}\left(\frac{R}{r}\right)^3 & r \geqslant R. \end{cases} \quad (15)$$

The enhancement of the time-like component of the axial current matrix elements by the meson-exchange currents [17,18] is denoted by $\epsilon_{\rm mec}$.

III. RESULTS AND DISCUSSION

The EXVAM results reveal a large variety of structures in both nuclei, ^{96}Y and ^{96}Zr. In ^{96}Y the wave function of the 0^- ground state is built out of a single spherical configuration characterized on the neutron side by 1 particle occupation of the $2s_{1/2}$ and 5.65 occupation of the $1d_{5/2}$ spherical orbital. It is worthwhile to mention that the EXVAM many-nucleon basis for the spin-parity 0^- states contains also prolate and oblate deformed configurations in the intrinsic system which dominate the structure of the excited 0^- states. The wave function for the 8^+ isomer in ^{96}Y indicates a mixing of different prolate deformed configurations, the main one representing 81% of the total amplitude. The EXVAM excitation energy of 1.653 MeV compares well with the experimental value of 1.541 MeV [19]. The calculated spectroscopic quadrupole moment of this state amounts to -97.3 $e$fm^2 (effective charge 1.2 for protons and 0.2 for neutrons) while the experimental value is $-98(11)$ $e$fm^2 [20]. In ^{96}Zr the EXVAM results indicate that triple shape coexistence is specific for the structure of the investigated 0^+ states. The lowest four 0^+ states in ^{96}Zr manifest variable, for some states strong, spherical, oblate, and prolate mixing. Table I illustrates the total contribution of different spherical, prolate, and oblate deformed configurations in the intrinsic system as percentage of the total amplitude. In the intrinsic system the β_2 deformation of the configurations building the structure of the lowest four 0^+ states varies from 0.03 up to 0.34 for the prolate ones and in between -0.24 and -0.29 for the oblate ones. It is worthwhile to mention that the lowest spherical projected configuration of the EXVAM basis is characterized by 5.6 particle occupation of the $1d_{5/2}$ neutron orbital. In Fig. 1 the EXVAM spectrum of the lowest four 0^+ states is compared to the experimental one [20].

The mixing of configurations with different intrinsic deformations in the structure of the wave functions for the 0^+ states in ^{96}Zr induces $E0$ transitions with significant $\rho^2(E0)$ values as it is illustrated in Table II. The experimental strength $\rho^2(E0;0_2^+ \to 0_1^+) = 0.0075$ (14) is almost three times weaker than the EXVAM value, while the other

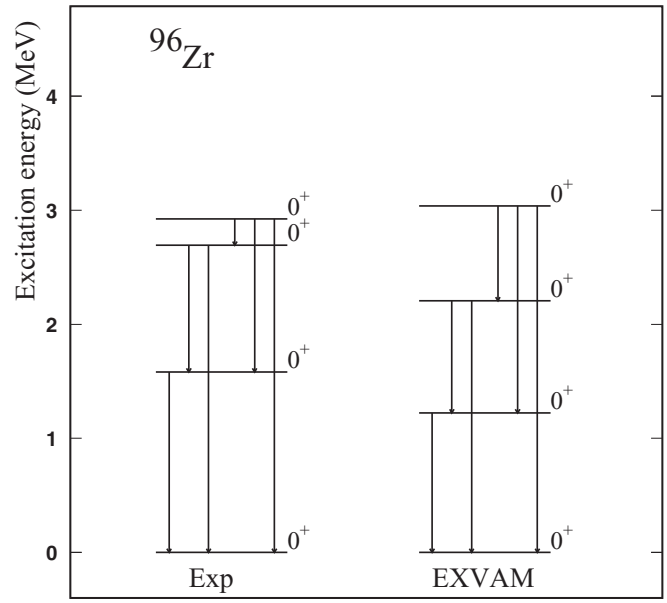

FIG. 1. The EXVAM spectrum of the lowest four 0^+ states in ^{96}Zr compared to data [20].

strengths $\rho^2(E0;0_3^+ \to 0_2^+)/\rho^2(E0;0_3^+ \to 0_1^+) = 9.4$ (2.6), $\rho^2(E0;0_4^+ \to 0_2^+)/\rho^2(E0;0_4^+ \to 0_1^+) < 3$ [20] indicate similar behavior as the theoretical results.

The structure of the calculated 8^+ states in ^{96}Zr indicates variable mixing of prolate and oblate deformed states in the intrinsic system. The spectroscopic quadrupole moments for the calculated lowest GT daughter states are depicted in Fig. 2. The calculated excitation energy of the yrast 8^+ state dominated (96%) by a prolate deformed configuration is 4.549 MeV, while the experimental value is 4.390 MeV.

The 7^+ states displaying the strongest branches in the Gamow-Teller strength distribution are dominated by one prolate deformed configuration. Higher lying states indicate oblate content varying from 3% to 68%, but the calculated GT branches are weak. The structure of the investigated 9^+ daughter states reveal a variable, in some cases strong, mixing of different prolate deformed configurations. The GT strength distribution for the decay of the 8^+ isomer to 9^+ states indicates weak branches making a very small contribution to the half-life. Figure 3 illustrates the EXVAM Gamow-Teller strength distribution for the decay of the 8^+ isomer in ^{96}Y to 8^+ states in ^{96}Zr and the data corresponding to the five states

TABLE II. $\rho^2(E0)$ values connecting the lowest four 0^+ states of ^{96}Zr.

Transition	EXVAM
$\rho^2(E0;0_2^+ \to 0_1^+)$	0.0215
$\rho^2(E0;0_3^+ \to 0_1^+)$	0.0048
$\rho^2(E0;0_3^+ \to 0_2^+)$	0.0525
$\rho^2(E0;0_4^+ \to 0_1^+)$	0.0084
$\rho^2(E0;0_4^+ \to 0_2^+)$	0.0104
$\rho^2(E0;0_4^+ \to 0_3^+)$	0.0155

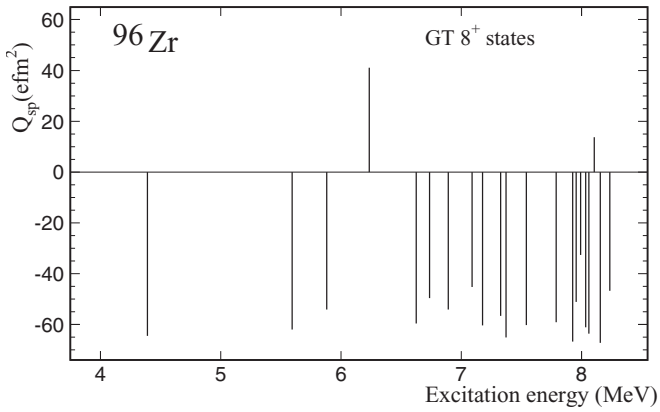

FIG. 2. Spectroscopic quadrupole moments of the 8^+ Gamow-Teller daughter states in ^{96}Zr.

assigned 8^+ or (7^+, 8^+) [20]. We assumed for the excitation energy of the yrast 8^+ the experimental value and for the other states the relative values with respect to this state. In Fig. 4 are presented the calculated Gamow-Teller strength distributions for the decay of the 8^+ isomer to 7^+ and 9^+ states in ^{96}Zr.

The analysis of the structure of the significant Gamow-Teller branches, the strongest being the one feeding the 8^+_1 state, indicates that significant contributions are coming from $g^{\nu}_{7/2}g^{\pi}_{9/2}$, $d^{\nu}_{5/2}d^{\pi}_{5/2}$, and $g^{\nu}_{9/2}g^{\pi}_{9/2}$ matrix elements. Smaller contributions are brought by the $d^{\nu}_{3/2}d^{\pi}_{5/2}$ matrix elements. For the decay to 7^+ states in ^{96}Zr the main contributions are brought by $g^{\nu}_{7/2}g^{\pi}_{9/2}$, $d^{\nu}_{3/2}d^{\pi}_{5/2}$, and $d^{\nu}_{5/2}d^{\pi}_{5/2}$ matrix elements. For the $8^+ \rightarrow 9^+$ relevant branches the contributing matrix elements are $g^{\nu}_{7/2}g^{\pi}_{9/2}$, $d^{\nu}_{5/2}d^{\pi}_{5/2}$, and $g^{\nu}_{9/2}g^{\pi}_{9/2}$. The weaker GT branches show cancellation of the contributions produced by these matrix elements. The *complex* excited Vampir half-life for the 8^+ isomer in ^{96}Y using the β window of $Q_{gg}(\beta^-) = 7.096$ MeV amounts to 9.3 s indicating agreement with the experimental value of 9.6 (2) s [20].

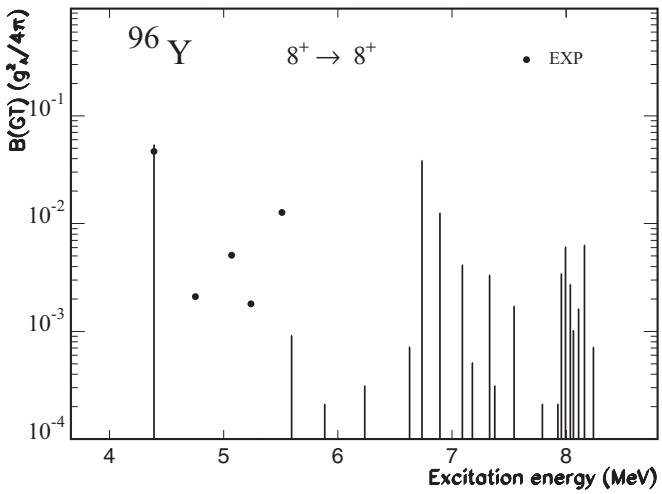

FIG. 3. The Gamow-Teller strength distribution for the decay of the 8^+ isomer in ^{96}Y to 8^+ states in ^{96}Zr obtained within *complex* excited Vampir model compared to data [20] (see text for details).

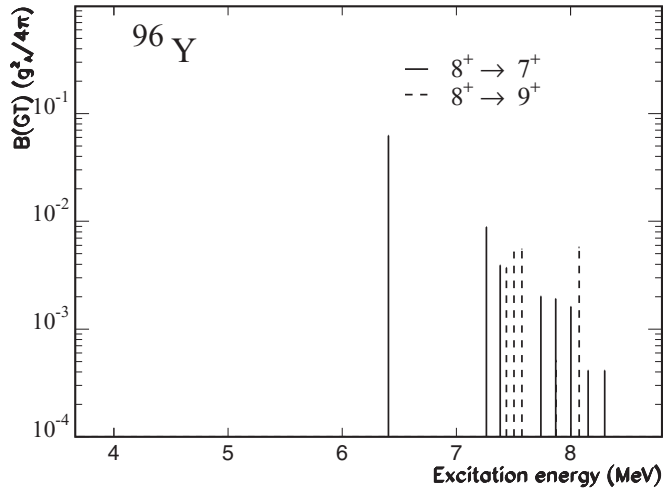

FIG. 4. The Gamow-Teller strength distributions for the decay of the 8^+ isomer in ^{96}Y to 7^+ and 9^+ states in ^{96}Zr obtained within *complex* excited Vampir model.

In the present work we calculated the first-forbidden $0^- \rightarrow 0^+$ decay branches of the ground state of ^{96}Y to the lowest four 0^+ states of ^{96}Zr taking into account the nuclear medium effect on the time-like component of the axial current using the meson-exchange enhancement factor $\epsilon_{\rm mec}$ while keeping the g_A value unquenched. The main contribution is brought by $s^{\nu}_{1/2}p^{\pi}_{1/2}$ matrix elements for all four 0^+ daughter states. Small canceling effects are introduced by the contribution of the $d^{\nu}_{3/2}p^{\pi}_{3/2}$ matrix elements. We present results for $\epsilon_{\rm mec} = 1.15$ giving the best comparison with the data and for a larger value, 1.19, illustrating the effect of an increased enhancement. The results for the logft values considering the EXVAM excitation energies of the four 0^+ daughter states in ^{96}Zr are presented in Table III. Taking into account the four decaying branches the calculated half-life of the 0^- ground state of ^{96}Y amounts to 5.21 s and 4.43 s for 1.15 and 1.19 enhancements of the axial-charge matrix element, respectively, while the experimental value is 5.34 (5) s.

IV. CONCLUSION

This work presents the first comprehensive results obtained within the beyond-mean-field *complex* excited Vampir model concerning the effects of triple shape coexistence identified in the structure of the 0^+ states in ^{96}Zr on their properties as well as on the first forbidden β^- decay of the 0^- ground state of ^{96}Y to the lowest four 0^+ states of ^{96}Zr. In the

TABLE III. The logft values for the decay of the 0^- ground state of ^{96}Y to the lowest four 0^+ states of ^{96}Zr compared to data [20].

$I[\hbar]$	$\epsilon_{\rm mec} = 1.15$	$\epsilon_{\rm mec} = 1.19$	Exp.
0^+_{gs}	5.60	5.53	5.59 (1)
0^+_2	6.40	6.32	6.97 (4)
0^+_3	6.52	6.45	7.41 (6)
0^+_4	6.48	6.42	7.92 (9)

frame of the same formalism, based on a realistic effective interaction and a large model space, we simultaneously described the Gamow-Teller decay of the 8^+ isomer in ^{96}Y to 8^+, 7^+, and 9^+ daughter states in ^{96}Zr. The comparison with the available data indicate good agreement giving support to our scenario on the evolution of the shape coexistence and mixing with increasing spin and excitation energy in both the odd-odd parent nucleus and the even-even daughter nucleus.

ACKNOWLEDGMENTS

This work has been supported by the Ministry of Education and Scientific Research (Romania), Program Nucleu No. PN-19060103.

[1] C. Y. Wu *et al.*, Phys. Rev. C **70**, 064312 (2004).
[2] G. S. Simpson *et al.*, Phys. Rev. C **74**, 064308 (2006).
[3] A. Petrovici, K. W. Schmid, and A. Faessler, J. Phys. Conf. Ser. **312**, 092051 (2011).
[4] A. Petrovici, K. W. Schmid, and A. Faessler, Prog. Part. Nucl. Phys. **66**, 287 (2011).
[5] A. Petrovici, Phys. Rev. C **85**, 034337 (2012).
[6] D. Jordan *et al.*, Phys. Rev. C **87**, 044318 (2013).
[7] E. Clément *et al.*, Phys. Rev. Lett. **116**, 022701 (2016).
[8] T. Rzaca-Urban *et al.*, Eur. Phys. J. A **9**, 165 (2000).
[9] M. Albers *et al.*, Phys. Rev. Lett. **108**, 062701 (2012).
[10] A. Petrovici, Phys. Scr. **92**, 064003 (2017).
[11] L. W. Iskra *et al.*, Europhys. Lett. **117**, 12001 (2017).
[12] M. Ichimura, H. Sakai, and T. Wakasa, Prog. Part. Nucl. Phys. **56**, 446 (2006).
[13] H. Behrens and W. Bühring, Nucl. Phys. A **162**, 111 (1971).
[14] T. Suzuki, T. Yoshida, T. Kajino, and T. Otsuka, Phys. Rev. C **85**, 015802 (2012).
[15] Q. Zhi, E. Caurier, J. J. Cuenca-García, K. Langanke, G. Martínez-Pinedo, and K. Sieja, Phys. Rev. C **87**, 025803 (2013).
[16] H. Behrens and W. Bühring, *Electron Radial Wave Functions and Nuclear β-Decay* (Clarendon, Oxford, 1982).
[17] H. Mach, E. K. Warburton, R. L. Gill, R. F. Casten, J. A. Becker, B. A. Brown, and J. A. Winger, Phys. Rev. C **41**, 226 (1990).
[18] J. Kostensalo and J. Suhonen, Phys. Lett. B **781**, 480 (2018).
[19] U. Hager *et al.*, Nucl. Phys. A **793**, 20 (2007).
[20] D. Abriola and A. A. Sonzogni, Nucl. Data Sheets **109**, 2501 (2008).